Thin Solid Films 671 (2019) 64–76

Contents lists available at ScienceDirect

Thin Solid Films

journal homepage: www.elsevier.com/locate/tsf

Atmospheric pressure plasma polymerization of organics: effect of the presence and position of double bonds on polymerization mechanisms, plasma stability and coating chemistry

J. Mertens[a], J. Baneton[a], A. Ozkan[a], E. Pospisilova[b], B. Nysten[b], A. Delcorte[b], F. Reniers[a,*]

[a] Chimie analytique et chimie des interfaces, Université Libre de Bruxelles, Campus de la Plaine, Batiment A, local A.3.1402, Boulevard du Triomphe, Brussels 1050, Belgium

[b] Institut de la matière condensée, Bio and Soft Matter, Institute of Condensed Matter and Nanosciences (IMCN), Université Catholique de Louvain, Boite L4.01.10 Place Louis Pasteur 1, Louvain-la-Neuve B3148, Belgium

ARTICLE INFO

Keywords:
Atmospheric dielectric barrier discharge
Polymerization mechanism
Organic coating
Double bond

ABSTRACT

Oxygen rich organic coatings are synthesized in a dielectric barrier discharge at atmospheric pressure. The critical effect of the precursor structure on the final chemical and physical properties of the synthesized coatings and the plasma characteristics are reported. A correlation is proposed between the electrical, optical emission spectroscopy and atmospheric mass spectrometry (MS) measurements of the plasma phase with the chemical properties of the synthesized films. It is shown that the addition of a precursor in an argon plasma leads to a stabilization of the discharge, critically dependent on the precursor structure itself. Different polymerization pathways are evidenced for the saturated and unsaturated precursors by the monitoring of some specific fragments by MS. The polymerized coatings are also characterized with X-Ray Photoelectron Spectroscopy, Infrared Spectroscopy and Atomic Force Microscopy. The presented results not only evidence a stronger preservation of the precursor structure with double bonds in the plasma phase but also reveal the essential role of the distance separating the unsaturation and a function of interest.

1. Introduction

Fiber reinforced epoxy resins have been widely used in the aeronautic and aerospace industries as thermosetting polymers [1–3]. Nevertheless, the more severe European environmental norms strongly force the scientific community to develop new materials to replace these epoxies such as the benzoxazines [4,5] and polyurethanes [6–7] which are seen as very promising alternatives. Therefore, optimal interface interactions between these resins and the 2024 aluminum alloy used in the aeronautic industry are an essential requirement. A possible solution is the plasma synthesis of an intermediate oxygen rich coating. Plasma has nowadays become a more and more common and suitable technique for the synthesis of various thin coatings on all kind of substrates. This method allows the elaboration of brand new polymers because of their different synthesis pathways when compared to the conventional polymerization [7]. Indeed, the highly energetic species initiated in the discharge – electrons, ions and metastables – induce a fragmentation of the precursors leading to an irregular polymer structure that could present a higher degree of cross-linking than the one of a conventionally reticulated polymer. Once synthesized, the surface properties can be tuned depending on the final application [8–10]. For example, the amount of polar groups can be drastically increased for the improvement of adhesion properties of further coatings.

Low pressure plasmas were widely used for the last decades in a very broad range of applications [11–14]. At low pressure, the larger mean free path of the different entities allows a very good reproducibility and prediction of the final properties of the synthesized coatings. On the other hand, the use of atmospheric pressure plasma is more recent and has the main advantage of avoiding the constraints of vacuum technology, which are very limiting in industry. These last years, organic and inorganic films were produced or post treated using several atmospheric plasma techniques [15–21]. Because of the smaller mean free path of the highly energetic species, working at atmospheric pressure induces an increase of the possible reactions occurring and formed moieties in the reactor lead to various coatings final properties and a relatively low reproducibility. A clear understanding of the polymerization mechanisms at atmospheric pressure is therefore very complex and remains one of the main challenges of the field.

* Corresponding author.
E-mail addresses: jermerte@ulb.ac.be (J. Mertens), freniers@ulb.ac.be (F. Reniers).

https://doi.org/10.1016/j.tsf.2018.12.036
Received 4 September 2018; Received in revised form 19 December 2018; Accepted 19 December 2018
Available online 21 December 2018

More specifically, the plasma polymerization of anhydrides has been studied in various systems such as pulsed radio frequency and continuous wave [22–26], microwave reactor [27] or dielectric barrier discharge (DBD) [28,29]. Their high oxygen content could lead to the synthesis of carboxyl rich coatings through the opening of the anhydride function in presence of moisture [30]. For example, the case of methacrylate anhydride has already been investigated for the synthesis of copolymers by the use of a pulsed plasma system [31] or for the synthesis of hydrolysis sensitive coatings by an aerosol assisted plasma process [32]. In addition, the use of several acid monomers is also reported in the literature. As example, Hegemann and al. investigated the low-pressure plasma polymerization rate of acrylic acid [33]. This monomer has also been used for several applications such as the formation of biocompatibles coatings [34] or surface composites [35].

The plasma polymerization mechanisms of double bonds containing monomers, such as ethyl lactate or allylamine, have been investigated at low pressure through the combination of computational simulations with the plasma phase and chemical analysis of the synthesized films [36–38]. At atmospheric pressure, several studies proposed a correlation between mass spectrometry (MS) or optical emission spectroscopy (OES) measurements with the chemical properties of the deposited films for acrylate compounds [39–41], fluorinated molecules [42] or vinyl ester resins [43].

In this work, we combine a plasma phase analysis with the chemical properties of the synthesized coatings at atmospheric pressure to better understand the effect of the presence and position of double bonds in 5 monomers: methacrylate anhydride (M.A.), isobutyric anhydride (I.A.), butyric acid (B.A.), crotonic acid (C.A.) and 3-butenoic acid (Be.A.). The method developed in our laboratory [39,44] combining atmospheric mass spectrometry of the plasma phase with an X-ray photoelectron spectroscopy (XPS) analysis of the deposited coatings is improved by the addition of OES, Fourier-transform infrared spectroscopy (FTIR) and atomic force microscopy (AFM) measurements. An electrical characterization recently reported in the literature [45] is also carried out in order to evaluate the changes in the electrical behavior of the plasma with the addition of the precursor and to monitor some important electrical parameters of the discharge (voltage, current, number of microdischarges…). A proper correlation between the plasma fragmentation and the chemical analysis of the coatings is proposed through the combination of these techniques.

2. Materials and methods

2.1. Materials

The influence of the double bonds in anhydrides is investigated with isobutyric anhydride and methacrylate anhydride provided by Sigma Aldrich. The effect of the position of the double bond is evaluated through the use of butyric, crotonic and 3-butenoic acid provided by Sigma Aldrich. The chemical structure of the precursors is presented in the Fig. 1. The plasma gas used is 99.99% pure argon (Air liquide). The coatings are deposited on a 1 mm thick aluminum 2024 T3 alloy provided by the SONACA Group.

2.2. Oscilloscope

Electrical measurements are performed via a digital oscilloscope Tektronix DPO 3032. The total current of the discharge is recorded using a Pearson 2877 Rogowski coil placed in serial connection with the DBD reactor. Power measurements are carried out via the Lissajous method [46]. For this purpose, both the applied high voltage (measured with a Tektronix P6015A probe) and the voltage across an external capacitor of 33 nF in series with the DBD reactor are monitored via the oscilloscope.

2.3. Atmospheric mass spectrometry

Atmospheric mass spectrometry of the plasma phase is performed with a Hiden analytical-QGA HAS-301-1106PL. The different gases are transferred from the reactor to the analyzer through a thin capillary placed into the plasma region between the two electrodes. A secondary electron multiplier detector allows to detect the fragments with low partial pressure (10^{-6}–10^{-13} Torr). The electron energy is set at 35 eV in the ionization chamber to avoid a too high fragmentation of the initial fragments. MASsoft7 software is used to analyze the partial pressure of various fragments defined by their m/z ratio as a function of the process time.

2.4. X-Ray photoelectron spectroscopy

The XPS analysis is performed with an ultra-high vacuum Physical Electronics PHI-5600 photoelectron spectrometer. The X-Ray source is a magnesium anode (1253,6 eV) operating at 200 W. The general composition of the surface of the sample is determined by a survey analysis where the spectra are acquired by averaging 7 scans at a 187.5 eV pass-energy and 0.8 eV/step. The C1s high resolution (HR) spectra, allowing the determination of the chemical environment of carbon, are acquired after the accumulation of 10 scans at a 23.5 eV pass-energy and 0.05 eV/step. The elementary composition and the deconvolution of the HR C1s spectra is calculated with the Casa XPS software after removal of a Shirley background and using the sensitivity coefficients given in the manufacturer's handbook: $S_O = 0.63$, $S_C = 0.205$, $S_{Al} = 0.11$. The C1s spectrum is here deconvoluted in four components: C—C (284.9 ± 0.1 eV), C—O (286.6 ± 0.1 eV) C═O (288.0 ± 0.1 eV) and O-C═O (289.0 ± 0.1 eV).

2.5. Profilometry

A Brücker Dektak XT stylus profiler is used for thickness measurements of the deposited coatings. It is equipped with a 2 µm radius stylus and is controlled and analyzed with the Vision 64 software. The thickness is calculated based on a step measurement between the coating and a scratch performed after the synthesis. The stylus strength used for these scans is set at 0.5 mg.

2.6. Atomic force microscopy

AFM images are recorded in air with a Bruker Icon Dimension microscope operating in Peak Force Tapping mode (PeakForce QNM). The probes are commercially available ScanAsyst probes with a spring constant of 0.5–0.8 N/m, a resonance frequency lying in the 70–95 kHz range and a typical tip radius of 2–12 nm. The 3D images are recorded with a sampling resolution of 512 × 512 data points and scan size of $3 \times 3\ \mu m^2$.

2.7. Infrared reflection absorption spectroscopy analysis (IRRAS)

FTIR analysis is performed on a Thermo Scientific Nicolet 6700 FTIR Spectrometer using a Reflection Absorption Spectroscopy technique (RAS). The spectra are acquired between 700 and 4000 cm^{-1} by the accumulation of 64 scans with a resolution of 4 cm^{-1}. The infrared signal is then computationally interpreted and analyzed by the OMNIC 8.1 software.

2.8. Optical emission spectroscopy

Optical Emission Spectroscopy was realized by collecting the emitted light of the discharge with a Spectra Pro-2500 I spectrometer from Acton Research. Comparisons between the peaks intensities in the absence and presence of the precursors were performed after normalization of the whole signal by the total intensity of the continuum

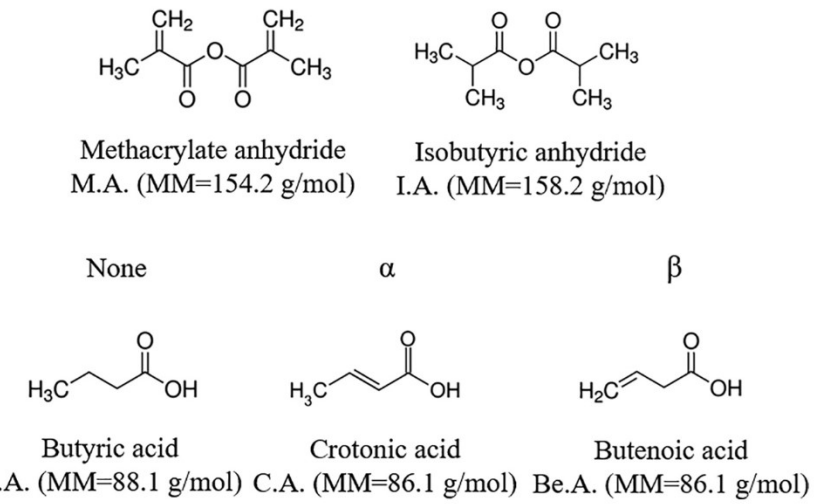

Fig. 1. Chemical structure of the anhydride and acid monomers used, their respective molecular mass and position of the double bond (for the acids).

between 200 and 900 nm. Spectra were acquired with a 1800 grooves/mm grating, the accumulation of 50 scans and an exposure time of 30 ms.

2.9. Experimental set up

The plasma polymerized organic films are deposited using a home-built DBD device. Both electrodes are copper disks of 45 mm diameter. A 2 mm thick pyrex dielectric (PierreGlas) is placed on the bottom electrode and a 3 mm thick α-alumina dielectric (Friatec) on the power one. The gap between the two electrodes is fixed at 4 mm to avoid any arc. In order to enhance the homogeneity of plasma polymerized films, the precursor is introduced in the plasma chamber using a ring diffusor directly in the discharge zone. A proper scheme of the reactor can be found in a previous publication [47].

The internal contamination of the reactor is minimized by pumping the gas down to a pressure of 270 Pa. The atmospheric pressure is then reached by filling in the chamber with argon and then, the precursor is introduced into the discharge by means of the carrier gas after being diluted with a primary flow. The total flow rate entering into the reactor is set at 6 L/min and the secondary flow rate is adapted following the amount of precursor needed to be injected.

The operating frequency is set at 17.1 kHz on the HV AFS-G10S power generator. Three different applied powers (30, 50 and 70 W) were throughout this work. The effective measured plasma power corresponds to 18, 31 and 43 W respectively, without the injection of precursor.

3. Results and discussions

3.1. Effect of the presence of double bonds in the injected precursor on the plasma and plasma deposited -coatings properties

3.1.1. Influence of the addition of precursors on the electrical and physical properties of the plasma phase

The influence of the addition of the precursors into the pure argon discharge on the electrical properties of the plasma is discussed below. The applied power and the total flow rate are set at 50 W and 6 L.min^{-1} respectively. The 25 mg.min^{-1} mass flow rate of precursor introduced into the discharge corresponds to a molar flow rate of 1.62×10^{-4} mol min^{-1} and 1.58×10^{-4} mol.min^{-1} for M.A. and I.A. respectively which allows the assumption of similar and so comparable amount of injected monomer into the discharge.

Fig. 2 shows the oscillograms of the plasma phase with and without the addition of precursor vapors. We observe that the pure argon discharge (black curve on the figure) exhibits a classical filamentary character, as reported in the literature [48]. When one of the investigated precursors is injected keeping the total gas flow rate constant at 6 L.min^{-1}, the electrical behavior of the discharge is drastically modified (see red and blue curves on the same figure). Indeed, one can observe an evolution from a truly filamentary discharge (pure argon) to a semi-homogeneous discharge (with the addition of precursor), which is also visually observed with naked-eye. The number of significant current peaks, calculated by a peak fitting method developed in a previous study [45], is decreased from 203 per half period in pure argon to 19 and 10 by the respective addition of I.A. or M.A.. In parallel, a strong modification of the average full width at half maximum (FWHM) of the peaks is observed by the addition of the anhydride molecules. The 52 ns average FWHM measured in the pure argon discharge increases up to 600 ns and 1026 ns when I.A. or M.A. are injected into the plasma respectively which is supporting the increase in homogeneity of the discharge (see Table 1. Kogelschatz et al. [49] explain that, in a filamentary regime, each short-lived microdischarge has an almost cylindrical plasma channel, (typically of about 100 μm radius)- a lifetime of a few nanoseconds, and spreads (in space and time) into a larger surface discharge close to the dielectric surface(s). The

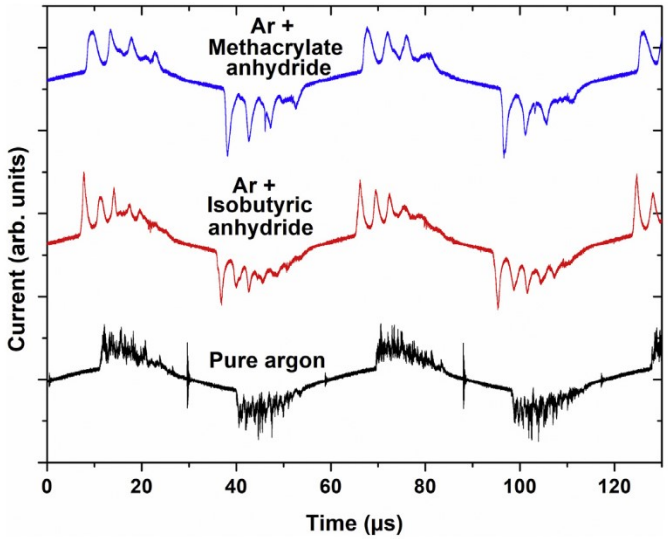

Fig. 2. Current profiles of the argon discharge with and without the addition of a 25 mg.min^{-1} flow of MA and IA. Applied power = 50 W and frequency = 17.1 kHz.

Table 1
Electrical analysis of the argon discharge with and without addition of 25 mg/min precursor with a 50 W injected power and a 17.1 kHz frequency.

Discharge gas composition	Number of significant peaks	FWHM(ns)	Effective power (W)	Voltage (V)	Current (mA)
Ar + M.A.	10 ± 2	1026 ± 56	29.4 ± 0.4	5205 ± 33	5.75 ± 0.14
Ar + I.A.	19 ± 3	600 ± 25	30.8 ± 0.3	5125 ±	6.06 ± 0.09
Pure Ar	203 ± 25	52 ± 3	31.3 ± 0.4	4988 ± 65	6.18 ± 0.12

radius of the microdischarge cylinder is highly dependent on the nature of the gas inside the discharge. Therefore, the addition of precursors could somehow induce a quenching with the argon metastable species and release some specific fragments which favors the stabilization of the discharge even for very low amounts. The sufficient overlapping of simultaneously propagating electron avalanches causes the smoothing of transverse field gradients and thus a stabilization of the discharge, which is the reason why the current peaks present at each half of period are relatively wider in the case of precursor addition. The decrease of the filamentary character of the discharge is quite interesting for the application since uniform plasma surface treatment is a desirable property if one wants to obtain homogeneous coatings.

The impact of the precursor nature on the effective discharge power, voltage and current is also evaluated by oscilloscope and the Lissajous method. It is observed that the injection of 25 mg/min M.A. leads to a decrease of 6.0% of the power effectively measured when compared to the pure argon discharge. In the case of I.A. a decrease of only 1.6% is observed. Even though a consistent trend is noted, the absolute current values must be taken into account with care because of the superposition of the error bars. As observed in Table 1, the decrease in effective evaluated power can be related to a decrease in current, whereas the plasma voltage is slightly increased. The discharge becoming less filamentary when injecting the precursor, a decrease in total current is logically expected and could be explained by the interactions between the highly energetic species, more specifically the electrons, and the injected monomer. The higher effect on the power, voltage, current and average FWHM with the monomer containing double bonds (M.A.) when compared to the saturated I.A. could be attributed to the higher interactions between the monomer and the plasma itself. Indeed, the higher absorption of electrons when double bonds are present (due to their higher reactivity) limits the current measured into the plasma but also leads to an increase of the measured voltage. B. Nisol & al recently developed a methodology to evaluate the energy effectively transferred from an argon discharge to a wide range of organic precursors. In good agreement with the present work, they reported a much higher energy transferred per injected molecule for unsaturated precursors [50–52].

(Fig. 3A) shows the optical emission spectra of the pure Ar discharge, and the Ar discharge with the two precursors. Apparently, no new emission lines or bands are observed when the precursors are injected into the discharge. Nevertheless, the comparison of the relative intensities, which correspond to a normalization through the integration of the whole OES signal, of the 763.5 nm Ar, 431.4 nm CH and the 310.0 nm OH lines, presented in (Fig. 3B), highlight significant variations when a precursor is injected into the argon plasma.

For the ease of the discussion below we decided to arbitrary fix the relative intensity of the Ar, CH and OH lines of the pure argon discharge to 100% and compare their relative signal intensity to this value when a precursor is injected into the plasma. When focusing on the emission of the 763.5 nm line corresponding to the Ar $3p^5 4p2p_6$-$3p^5 4p1s_5$ transition, one can see that the addition of 25 mg/min of monomer leads to a decrease of the relative intensity of the major argon line. As the intensity of a line in OES reflects the population of the excited level, this suggests that when a monomer is added in the discharge, the amount of energy initially transferred for the excitation of the argon is lowered, decreasing the population of the excited state and the observed emission. The evaluated emission reduction of the Ar line at 763.5 nm, representative of the behavior of all the Ar lines, with the introduction of precursor might be related to quenching between the argon metastable species and the injected monomers. In the early 70s L.G. Piper [53,54] showed that the quenching rate of several argon metastable species with the injected precursor is critically dependent on the latter's cross section, size but also on the presence of unsaturations. He showed for instance that the injection of acetylene, induced a 17%, 50% and 25% increase of the quenching rate of the $Ar(^3P_2)$, $Ar(^3P_1)$, $Ar(^1P_1)$ metastable species respectively when compared to the saturated ethane. A stronger decrease of the relative intensity of the Ar line at 763.5 nm is observed when the methacrylate anhydride is used. This could indicate a more important energy transfer between the argon discharge and the monomer possibly associated to the higher reactivity of the double bonds which can be correlated to the current, effective power and potential values presented in Table 1. When giving a closer look to the emission of the CH and OH signals, which shouldn't be observed in an ideal pure argon discharge but difficult to avoid at atmospheric pressure despite the pumping processes limiting the contaminations, it is noted that the chemical structure of injected monomer induces strong variations in their relative emission intensity when compared to a pure argon discharge. Both lines intensities are increased by the addition of the precursors which is easily understandable since they could be considered as major providers of the species emitting at 431.4 nm and 310.0 nm. Nevertheless, the CH and OH emission lines are more critically increased when the saturated monomer (I.A.) is injected. In other words, the injection of the M.A. seems to limit the amount of CH and OH emissive fragments into the discharge which suggests a different kind of interaction between the argon discharge and the injected precursor. This represents a first clue for various atmospheric plasma polymerization pathways. Their strong involvement in the I.A. polymerization mechanisms seems limited for M.A.

A better understanding of the fragmentation of the precursors into the discharge was achieved by MS measurements. We therefore analyzed the fragments of the precursor obtained without plasma, related to the fragmentation in the ionization chamber of the mass spectrometer, and those with a 50 W applied power discharge. Numerous signals related to the fragmentation of both precursors, also named "small fragments" are evidenced: CH_3^+ ($m/z = 15$), O^+/CH_4^+ ($m/z = 16$), CO^+ ($m/z = 28$), CO_2^+ ($m/z = 44$). Furthermore, we highlighted several medium size signals specifically associated to methacrylate anhydride: $C_3H_5^+$ ($m/z = 41$) and $C_4H_5O^+$ ($m/z = 69$) and to isobutyric anhydride: $C_3H_7^+$ ($m/z = 43$) and $C_4H_7O^+$ ($m/z = 71$) which can be explained by the presence or absence of the double bonds. The $C_4H_6^+$($m/z = 72$) fragment, specific of a plasma polymerization through the double bonds is also followed.

The partial pressures related to several small fragments, presented in Fig. 4, show that the 50 W plasma leads to a similar behavior regardless the injected precursor. Indeed, in both cases, when the plasma is lightened the number of small fragments is increased because of the precursor's fragmentation into the discharge. However, this increase is much more important in the case of isobutyric anhydride where the intensity of the signal associated to the small fragments (CH_3^+, CH_4^+/O^+ and CO^+) is raised by a factor of 5.0, 2.5 and 2.5 respectively. In the case of the methacrylate anhydride, where unsaturations are present, the intensity of the signals related to the small fragments is increased by approximately 30%. This suggests that the polymerization process of the isobutyric anhydride is more strongly associated to a fragmentation of the precursor than the methacrylate anhydride where

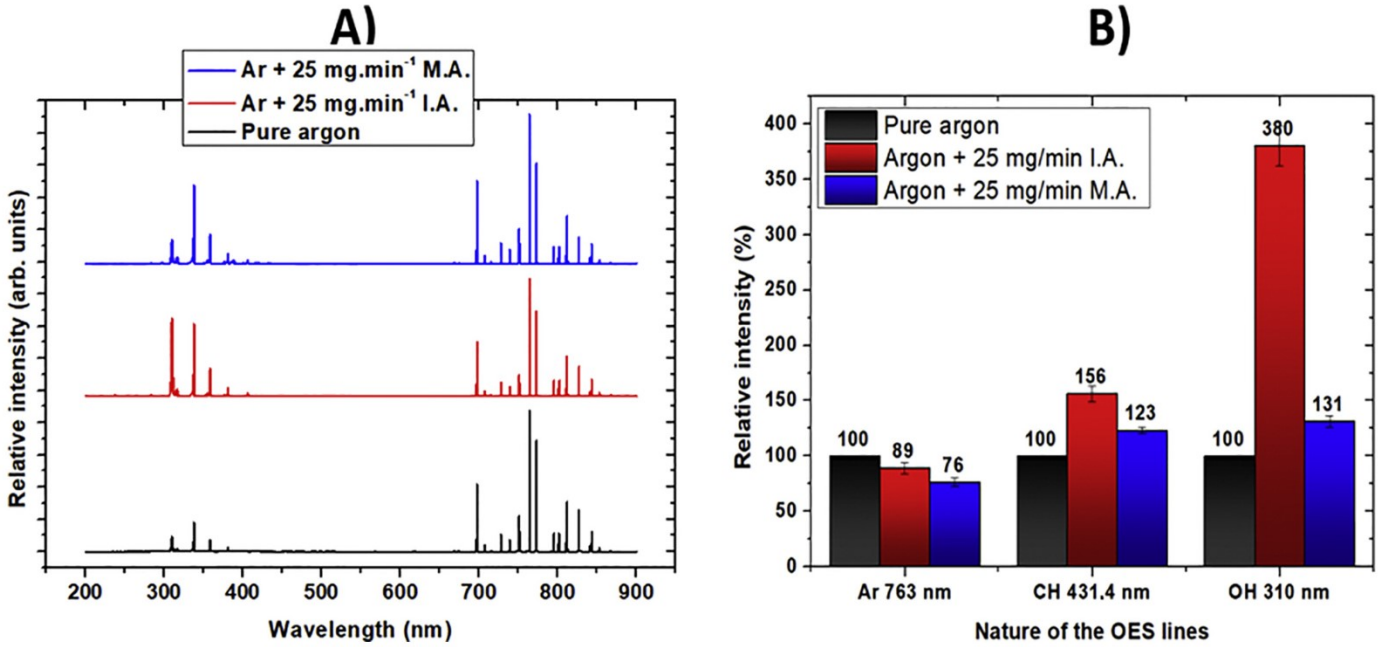

Fig. 3. (A) OES spectra of the pure argon discharge with and without addition of 25 mg/min I.A. and M.A. (B) Relative intensity of the 763.5 nm Ar, 431.4 nm CH and 310.0 nm OH lines observed by OES of a pure argon discharge with and without addition a 25 mg/min flow rate of M.A. and I.A. (the OH and CH lines in "pure" argon plasma are due to traces of contaminants which are hardly avoidable at atmospheric pressure).

the presence of double bonds seems to prevent the breaking of the chemical structure. Also, the stronger reduction of the filamentary character of the discharge with the M.A. could be partially responsible for the lower degradation of the precursor structure. This observation can be correlated to the OES relative emission intensity of the CH and OH lines and strongly support the importance of the fragmentation in their respective atmospheric plasma polymerization pathways.

This tends to be confirmed with the different behavior for the medium sized fragments ($C_4H_5O^+$, $C_3H_5^+$, $C_4H_7O^+$ and $C_4H_7^+$). As shown in Fig. 5, the intensity of the signals associated to these groups when the I.A. is injected ($C_4H_7O^+$ and $C_4H_7^+$) is strongly decreasing. Since the presence of these groups can be related to the partial preservation of the initial precursor's structure, their decrease when the plasma is lightened can thus be associated to a strong fragmentation

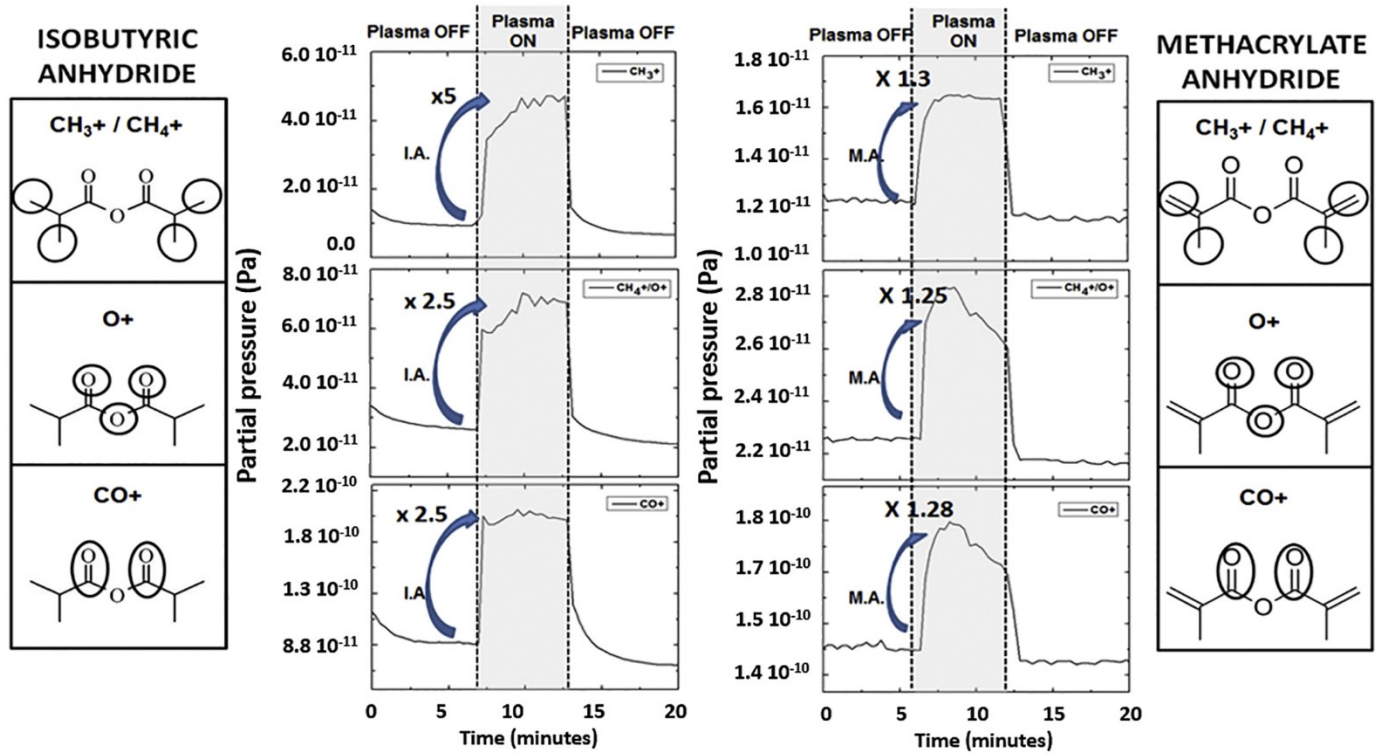

Fig. 4. Follow up and origin of the CH_3^+, CH_4^+/O^+ and CO^+ small fragments by mass spectrometry before, during and after lightening of the argon discharge with the addition of a 25 mg/min flow of M.A. and I.A.

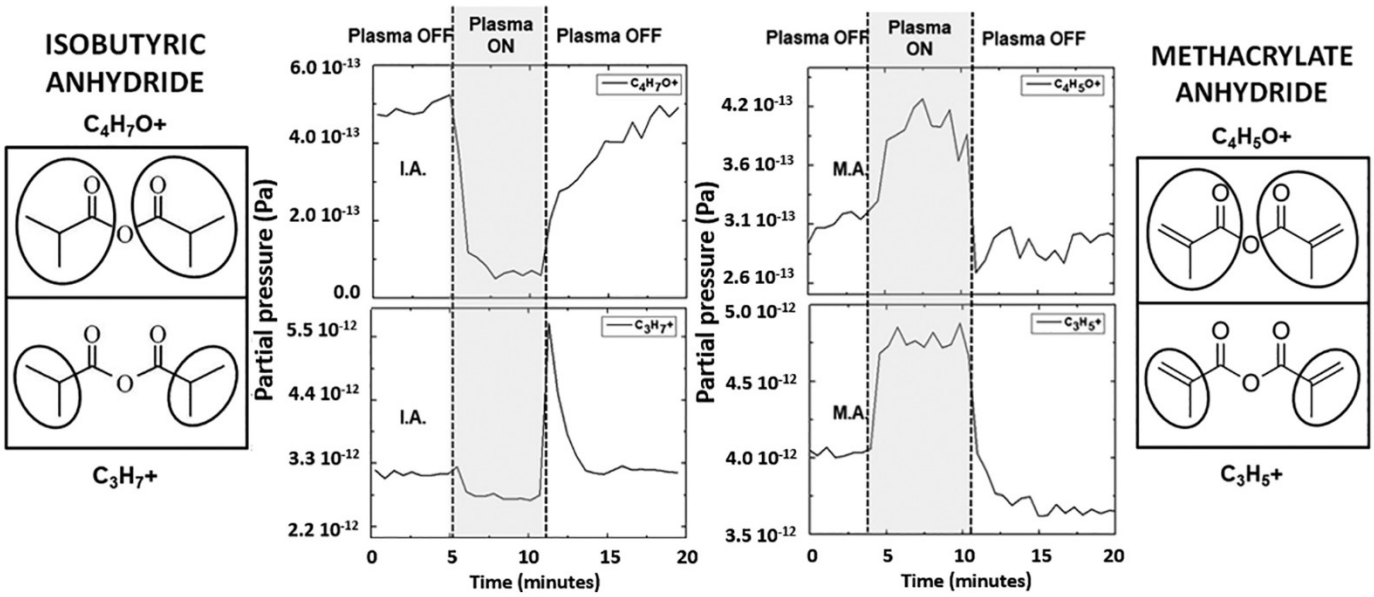

Fig. 5. Follow up and origin of the specific $C_4H_7O^+$, $C_3H_7^+$, $C_4H_5O^+$ and $C_3H_5^+$ medium size fragments by M.S. before, during and after lightening of the argon discharge with the addition of a 25 mg/min flow of M.A. and I.A.

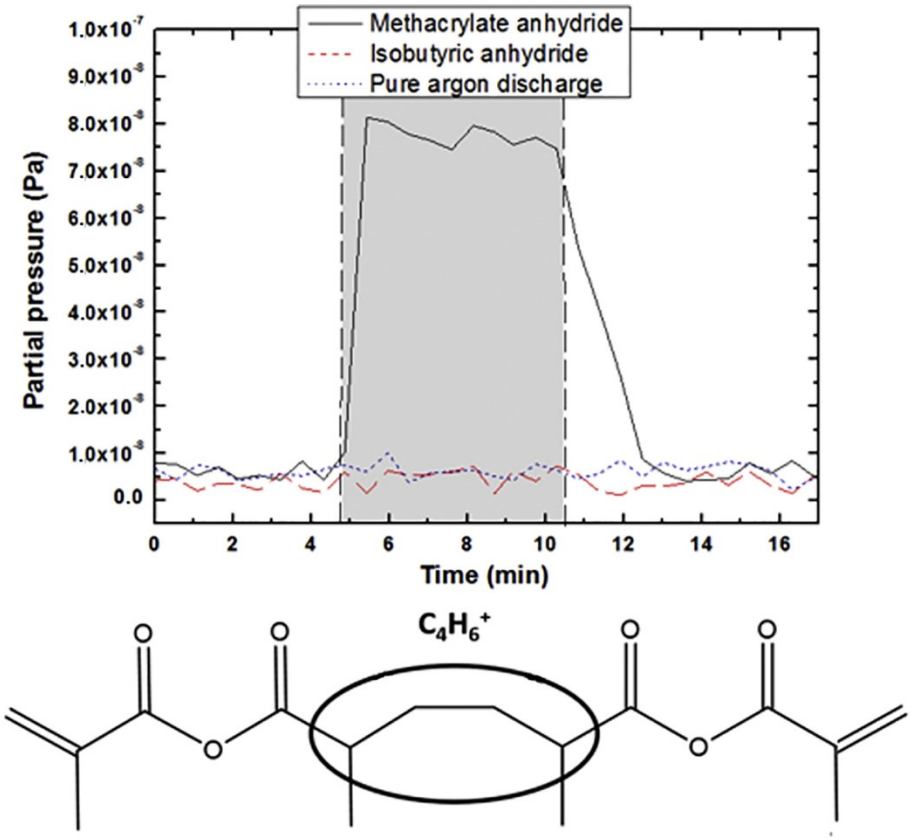

Fig. 6. Monitoring of the $C_4H_6^+$ fragments by M.S. before, during and after lightening of the argon discharge with the addition of a 25 mg/min flow of M.A. and I.A.

observed previously in Fig. 4 with the I.A.. For M.A., the plasma ignition favors the formation of these medium sized fragments which can be possibly observed by simple C—O or C—C bond breaking. Here, a respective 33.3 and 15.8% increase of the $C_3H_5O^+$ and $C_3H_5^+$ groups is noted suggesting, again, a limited fragmentation when compared to the I.A.. These observations must be associated to the follow up of a specific signal possibly related to a signature of the polymerization through the double bond in the plasma phase: $C_4H_6^+$. One can observe on Fig. 6 that before the activation of the plasma, the partial pressure associated to this specific fragment is not influenced by the presence or absence of any precursor. It is therefore assumed that the noise observed between 0 and 5 min indicates a total absence of the $C_4H_6^+$ fragment. When the plasma is ON, between 5 and 10 min, no change of the noise is observed for the pure argon discharge, easily understandable since no monomer is injected, nor for the I.A. which support the absence of this specific fragment. On the contrary, when M.A. is injected, the $C_4H_6^+$ signal

intensity is critically increased when the plasma is lightened. Since this fragment is absent of the initial chemical structure of the monomer, it can be considered as a signature of the polymerization through the double bonds into the plasma phase when the methacrylate anhydride is used as precursor. This observation clearly supports the proposition of the formation of oligomers into the plasma and thus the polymerization pathway dominated by the propagation of the radical character through the double bonds. The formation of these oligomers could now explain the increase of signal of the medium sized fragments (Fig. 5) because of the more important amount of moieties at their origin into the ionization chamber but also maybe to their longer lifetime in the mass spectrometer.

3.1.2. Chemical and physical characterization of the atmospheric argon plasma synthesized coatings

Since the effect of the injection of the precursors on the plasma phase properties has been discussed, the chemical and physical properties of the coatings deposited in similar conditions are evaluated by XPS, IRRAS, AFM and profilometry. For a clear correlation between the results presented in the previous section and the upcoming one, the following part will be separated in two main sections: i) The influence of the presence of the double bonds on the physical and chemical properties of the coatings ii) The use of double bonds for a better resistance of the precursor structure against the discharge power. All the deposited films are synthesized in a 50 W argon plasma at atmospheric pressure with the injection of 25 mg/min of precursor and a total gas flow rate of 6 L.min^{-1} during 3 min.

3.1.2.1. Influence of the presence of unsaturations in the precursor structure. XPS analysis reveals that the nature of the injected precursor has a significant impact on the surface chemical composition of the synthesized coatings. Indeed, I.A., impossible to polymerize using classical techniques, leads to a general surface chemical composition of 83.0% of carbon and 17.0% of oxygen whereas M.A. provides a coating composition of 76.5% carbon and 23.5% of oxygen. The composition of the coatings obtained with the latter precursor is very close to the one of the methacrylate anhydride left dry and polymerized in ambient air on the aluminum substrate for 24 h (carbon: 75.0% and oxygen: 25.0%). Fig. 7 presents the XPS C1s high resolution spectra of the conventionally and plasma synthesized coatings. These curves are deconvoluted in 4 components for an optimized fitting: C−C (284.9 ± 0.1 eV), C−O (286.6 ± 0.1 eV), C=O (288.0 ± 0.1 eV) and O-C=O (289.0 ± 0.2 eV).

It is observed that the average chemical environment of the carbon in the coatings synthesized using methacrylate anhydride as precursor is very similar to the one polymerized in conventional conditions. In comparison, it seems that when using I.A., the plasma synthesis leads to a lower preservation of the precursor initial structure. The oxygenated/branched components ratio (O/B_{ratio}) which can be defined as:

$$O/B_{ratio} = \frac{\%_{C-O} + \%_{C=O} + \%_{O-C=O}}{\%_{C-C}}$$

varies from 0.47 for the M.A. polymerized in ambient air to 0.45 and 0.34 for the plasma polymerized M.A. and I.A. respectively. This supports again that the polymerization pathways between the two precursors are quite different as it was discussed it in the first part of this study. It is assumed that the presence of the double bonds allows two types of polymerization: 1) A conventional one led by the radical propagation, initiated by the plasma and evidenced by the specific $C_4H_6^+$ fragment in the MS analysis, among the monomer's double bonds which seems to be dominant and 2) a polymerization induced by the fragmentation/recombination of the precursor which is here significantly limited. In the case of I.A. only the latter polymerization pathway is envisaged since no formation and propagation of the radical character is possible without the breaking of a chemical bond. The COOR component of the C1s XPS signal, which can be associated to the anhydride function, is the most affected one during the plasma synthesis of the coating with I.A. as precursor. On the contrary, its very good preservation with the methacrylate anhydride indicates a protective role of the double bond on the function of interest. In correlation with the results of the first part of this paper, we can assume that the higher reactivity of the double bond makes it a privileged target for the energy transfer between the highly energetic species and the monomer and reduce its degradation and fragmentation. In their recent papers, Loyer & al. used the combination of a chemical analysis of the synthesized coatings and DFT measurements to understand the atmospheric pressure plasma induced chemical vapor polymerization kinetic of acrylate precursors. They related the preservation of the chemical structure of the precursor to the presence of low bond dissociation energy groups (epoxyde in their case) which are considered as privileged target for the fragmentation. The present work is therefore in good agreement with their observations since the opening of the Π bond in the unsaturation has the lowest bond dissociation energy in the investigated precursors [55–57].

Since the synthesis duration is a fixed parameter, average deposition rates of the coatings can be evaluated by the profilometry measurement

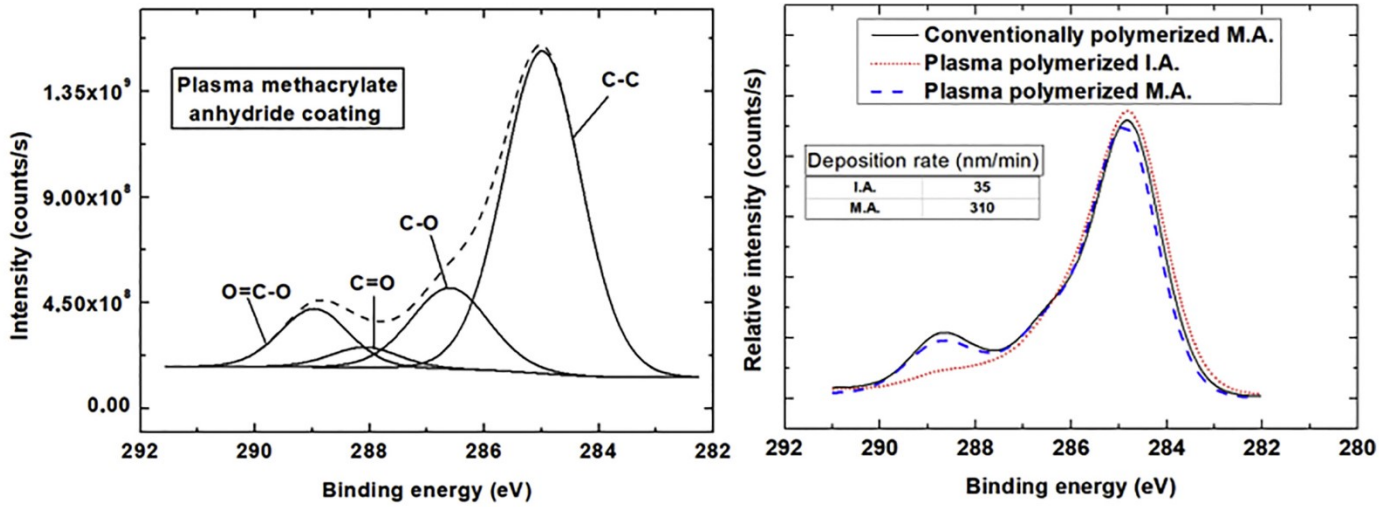

Fig. 7. Left: C 1 s High Resolution (HR) spectra of a methacrylate anhydride plasma synthesized coating at 50 W during 3 min and its deconvolution. Right: C 1 s HR spectra of the plasma polymerized isobutyric anhydride and methacrylate anhydride and their respective deposition rate compared to the conventionally polymerized methacrylate anhydride.

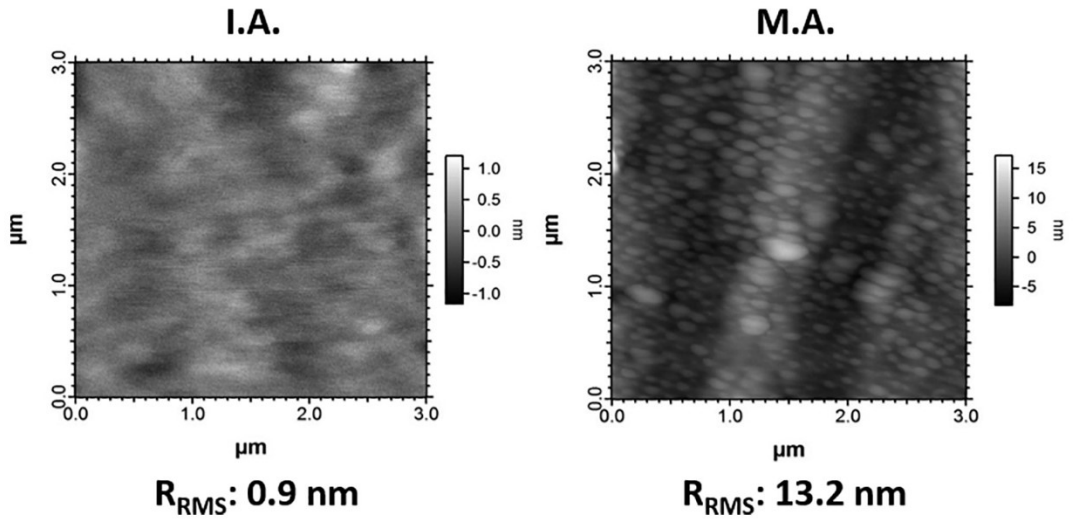

Fig. 8. 3 × 3 µm^2 AFM images of Al 2024 substrate covered by the plasma synthesized coatings at 50 W during 3 min using isobutyric anhydride (left) and methacrylate anhydride (right) as precursor.

of their respective thickness, assuming dense coatings. A nine time increase of the deposition rate induced by the presence of unsaturations in the monomer is highlighted (M.A.: 310 nm/min and I.A. 35 nm/min). This range of influence related to the presence of double bonds was already noted for acrylates and fluorinated compounds in similar reactors [42]. We assume that this significant difference can be explained by the higher reactivity of the double bonds but also by the double polymerization pathway which was suggested earlier for the methacrylate anhydride. AFM images, presented in Fig. 8, show that using I.A. as precursor leads to a relatively smooth coating with a Root Mean Square Roughness (R_{RMS}) evaluated at 0.9 nm whereas, on the contrary, M.A. coatings present a more important roughness with a R_{RMS} of 13.2 nm. This can be related to the different polymerization mechanisms of the two precursors within the plasma phase but also to their respective interaction with the substrate related to their vapor pressure which can be evaluated at 10.0 and 90.0 Pa at 20 °C for I.A. and M.A. respectively as reported in the literature [53].

IRRAS analysis is performed to study the bulk composition of the synthesized coatings (Fig. 9). It is noted that the signals associated to the CH_x stretching observed at 2970, 2937 and 2877 cm^{-1} are more important when compared to the C═O stretching observed between 1704 and 1800 cm^{-1} in the case of the I.A. plasma coatings. Indeed, this CH_x/C═O stretching ratio is 1.31 in the case of I.A. whereas it is evaluated at 0.58 in the case of M.A. plasma coatings. This lower ratio for M.A. indicates again a better preservation of the function of interest in the precursor and a less important fragmentation. Furthermore, a peak at 1643 cm^{-1} associated to the C═C stretching observed in the M.A. coatings suggests that the total amount of double bonds is not consumed during the plasma polymerization leading to a partially unsaturated polymer.

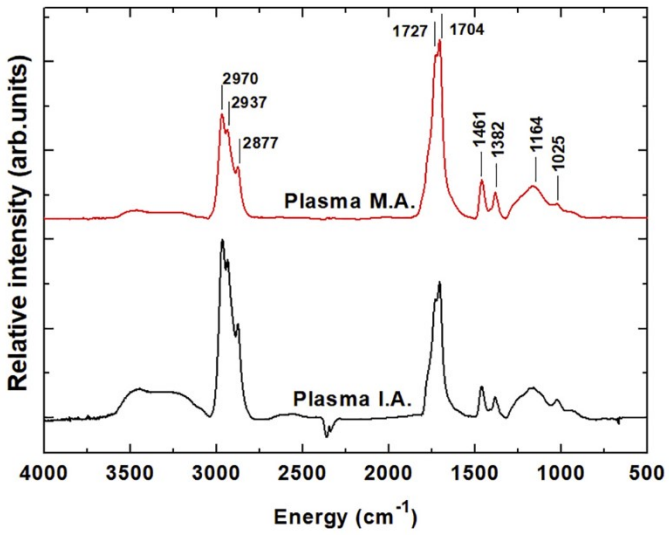

Fig. 9. IRRAS spectra of the plasma synthesized coatings at 50 W during 3 min using methacrylate anhydride and isobutyric anhydride as precursors and respective roughness.

3.1.2.2. Double bonds: protective tool of the function of interest against the discharge power. Usually, higher applied power is associated with a more important electron density into the discharge. When their number is increased, those highly energetic species, accelerated by the applied potential, can induce more fragmentation of the precursor. Here, 25 mg/min of monomer are injected in an argon discharge with a 30 W, 50 W and 70 W applied power. The C1s high resolution XPS spectra of the synthesized coatings are presented in Fig. 10. One can observe that in both cases, the amount of oxygenated species (O-C═O, C═O and C—O) decreases when the discharge power is increased which corresponds to a loss of the function of interest and a degradation of the precursor structure. Nevertheless, this loss in oxygenated species is more significant in the case of I.A. where the oxygenated/branched components ratio varies from 0.41 at 30 W to 0.30 at 70 W corresponding to a 25% decrease). This ratio varies from 0.51 at 30 W to 0.47 at 70 W associated to a 8% decrease when M.A. is used as precursor.

These results can be correlated to the infrared measurements presented in Table 2 where it is observed that the CH_x/CO ratio increases with the applied plasma power. This variation from 0.90 to 1.70 and 0.43 to 0.65 when applying a power between 30 W and 70 W when using I.A. and M.A. respectively is the result of a higher fragmentation of the precursor. It is important to note that this increase of CH_x/CO ratio with power is more significant in the case of I.A. indicating a lower preservation of the anhydride function and a higher fragmentation of the precursor compared to the M.A. This suggests that the presence of the double bonds leads to a better preservation of the precursor's structure in the plasma phase when increasing the applied power. Many hypotheses could be drawn to explain this behavior, and only a few ones will be developed here: a) the double bonds could be seen as privileged targets for the high energy electrons because of their higher reactivity. The energy needed for breaking the π-bond of the double bond, estimated at 2.70 eV, is making them the most probable

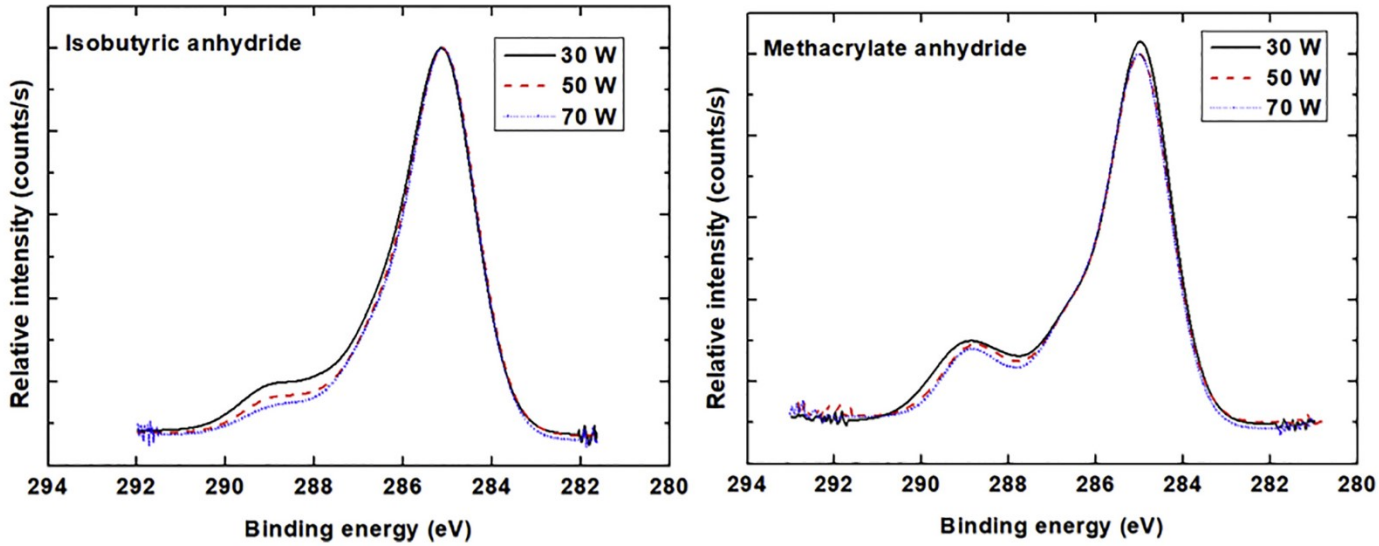

Fig. 10. C 1 s HR spectra of the plasma synthesized coatings during 3 min with isobutyic anhydride (left) and methacrylate anhydride (right) as liquid precursor at various discharge power.

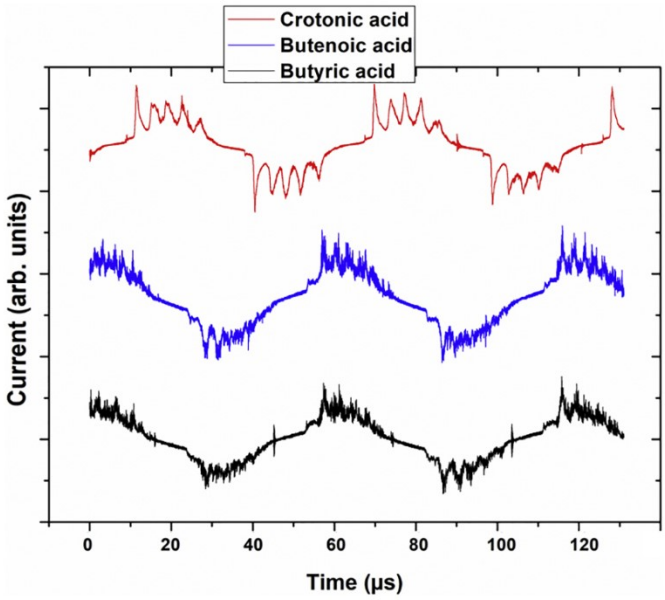

Fig. 11. Current measurement of the 50 W argon discharge with the addition of 25 mg.mn^{-1} of the butyric, crotonic and 3-butenoic acid.

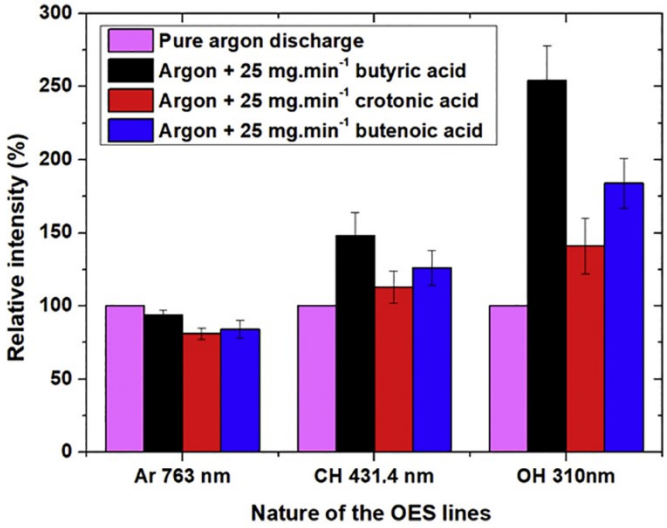

Fig. 12. Relative intensity of the Ar (763.5 nm), CH (434.1 nm) and OH (310.0 nm) lines of a pure 50 W argon discharge and with the injection of 25 mg.min^{-1} butyric, crotonic or 3-butenoic acid.

broken bonds when compared to the C—O and C—C bonds energy evaluated at 4.00 eV and 3.85 eV [58] respectively; b) as seen in the electrical part of this study, the number of streamers strongly decreases when injecting the precursors in the argon discharge, with a higher effect for M.A. The effective plasma power is also smaller with M.A. than with I.A. The energy inside the plasma being smaller with M.A., one can reasonably assume that the more fragile anhydride function is better preserved when the double bonds are present. Evidence of the capture of the energetic electrons by the C=C double bonds is indirectly given by the polymerization process proposed in this paper where the presence of the $C_4H_6^+$ fragment in mass spectrometry evidences the opening of the C=C double bond.

3.2. Effect of the position of the double bond on the protection of a function of interest

Since the importance of the presence of an unsaturation for the protection of a function of interest has been discussed hereabove, this part aims to go further in the discussion and report the influence of the position of the double bond on its protective effectiveness. Therefore, three acid monomers depicted in the Fig. 1 were used. A 25 mg/min^{-1} flow of monomer is injected in a total 6 L.min^{-1} argon flow rate and the applied discharge power is set at 50 W.

3.2.1. Plasma phase analysis

As observed in Fig. 11 and similarly to M.A. and I.A., the injection of the three acidic monomers reduces the amount of micro-discharges in the argon plasma from 203 to 183, 123 and 41 noted streamers for B.A., Be.A. and C.A. respectively. The lower decrease of the filamentary character of the plasma with the three monomers when compared to the anhydrides previously studied can be attributed to their higher C/O ratio. The breaking of bonds is assumed to be responsible for energy transfers between the discharge and the monomer inducing its stabilization. Yet the nature of the species relieved in the plasma plays a significant role on the physical properties of the discharge. More specially, the electrical properties of argon plasmas are known to be

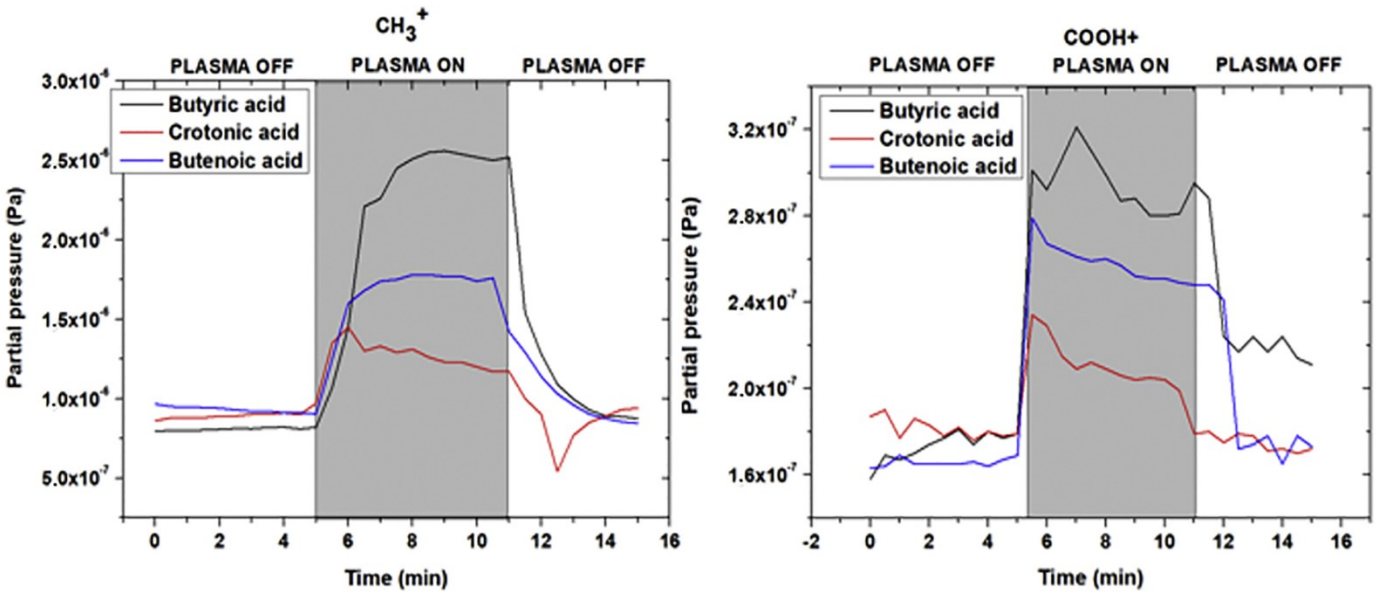

Fig. 13. Mass spectrometry tailoring of the CH_3^+ (m/z = 15) and COOH+ (m/z = 45) fragments before, during and after the plasma lightening.

modified by the addition of electronegative species such as oxygen and OH [59–62]. The injection of 25 mg.min^{-1} of each precursor induces the introduction of 1.2 10^{-3} and 5.8 10^{-4} mol of carbon and oxygen respectively where it could be evaluated at 1.3 10^{-3} and 4.910^{-4} for the anhydrides. Since the electrical properties of a discharge depends on the electron density but also on the nature of the species present into the plasma, the higher concentration of oxygen with acidic monomers might explain the lower stabilization than for anhydrides. Assuming this hypothesis, a double phenomenon can be considered in the case of the unsaturated monomers. Firstly, the higher reactivity of the C=C bond induces a more efficient energy transfer between the energetic species and the monomer limiting the excitation of the argon. This induces a stabilization of the plasma. Second, the possible resonance through the unsaturations inside the monomer limits the fragmentation of the acid function releasing less oxygen containing groups in the discharge such as the OH species.

A specific focus on the variation of intensity with the injection of the monomers is given to the CH, OH and Ar OES lines and reported in Fig. 12. As it was the case for I.A. and M.A., the injection of a precursor induces a decrease of the relative intensity of the Ar 763.5 nm line which could be related to energy transfers and electrons attachment to the monomers limiting the emission of the excited state of argon. The higher reactivity of the double bond can again explain a stronger reduction of the Ar 763.5 nm emission but no evident difference is noted with the position of the double bond for this line. An equivalent energy transfer from the discharge to both monomers can then be envisaged. The increase of the CH and OH lines can easily be related to the addition of monomers at the origin of these fragments. Even though similar trends are observed for the increase of these specific lines with the presence of unsaturation, a systematic different behavior is noted when the unsaturation is located in α or β of the function of interest. The emission of these lines is indeed less increased with the crotonic acid when compared to the butenoic acid. The CH line related to the fragmentation of the precursor indicates a better preservation of the structure of the crotonic acid. On the other hand, the OH line can be attributed to the fragmentation of the function of interest which is then also better preserved when the double bond is located in the alpha position. One possible explanation lies in the higher stability of the crotonic acid because of the possible resonance effect through the sp^2 carbons and its geometrical planarity. The lower emission of the fragmented species could also be at the origin of a more effective decrease of the filamentary character of the discharge as observed through the

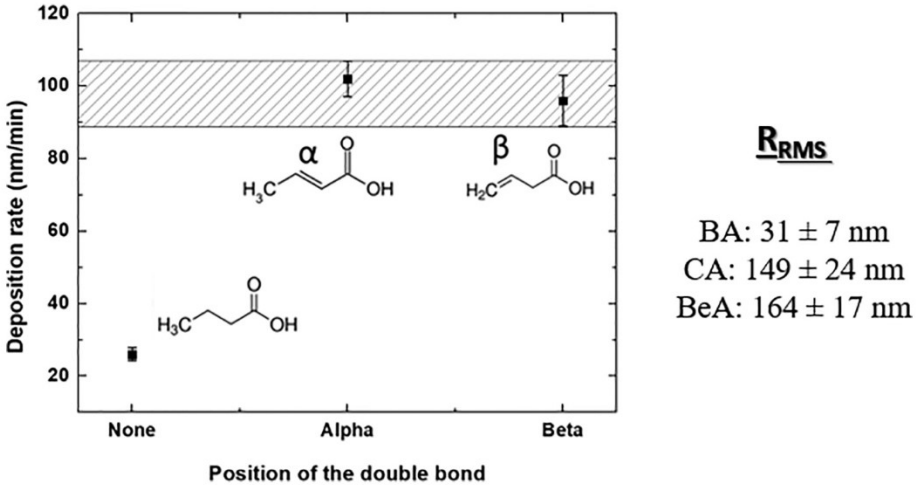

Fig. 14. Deposition rate of the monomers in a 50 W argon discharge with a 25 mg.min^{-1} flow rate of precursor and the respective roughness of the 300 nm thick coatings synthesized in similar conditions.

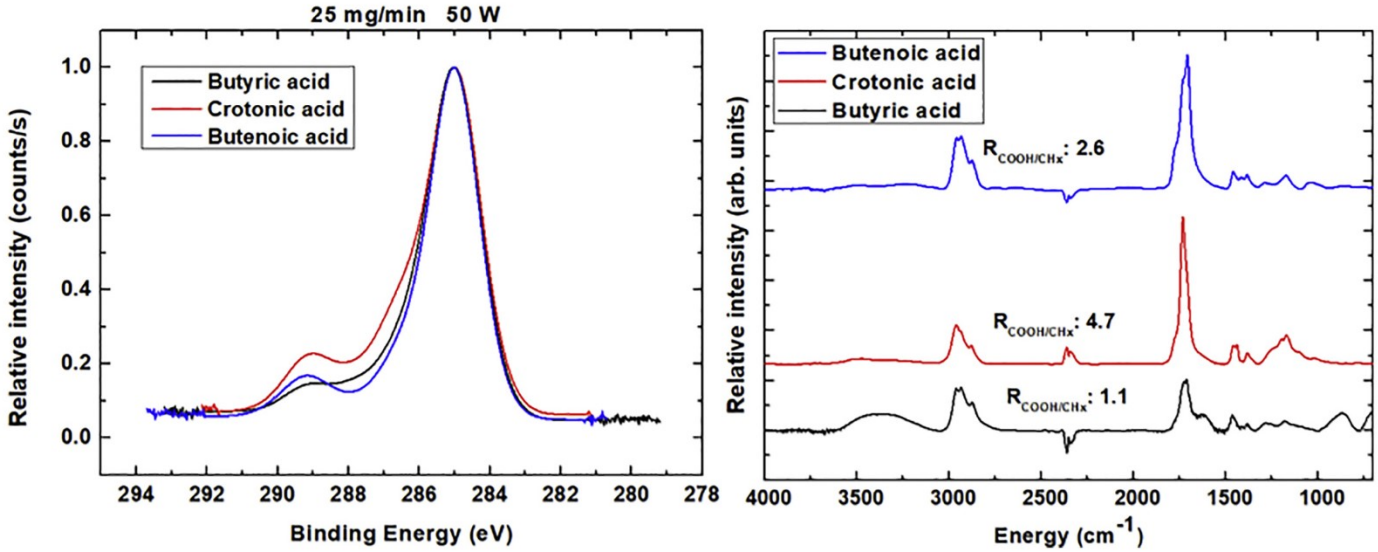

Fig. 15. XPS HR C1s (left) and IRRAS (right) spectra of the films synthesized by a 25 mg.min-1 introduction of monomer in a 50 W argon discharge.

Table 2
Evolution of the IRRAS CHx/C=O ratio in the plasma synthesized coatings using methacrylate anhydride and isobutyric anhydride as precursor and the effective discharge power with the injected power.

Injected power (W)	Methacrylate anhydride		Isobutyric anhydride	
	CHx/C=O ratio	Effective power (W)	CHx/C=O ratio	Effective power (W)
30	0.43	16.6	0.93	17.1
50	0.58	29.4	1.31	30.8
70	0.65	41.7	1.73	43.0

oscilloscope measurements.

The stability of the precursor in the discharge is evaluated by the tailoring of several selected fragments by mass spectrometry: CO_2^+ ($m/z = 44$), CH_3^+ ($m/z = 15$) and $COOH^+$ ($m/z = 45$). The results, presented in Fig. 13, indicate similar behaviors for the three monomers. The fragmentation of the precursor in the argon plasma can be qualitatively quantified by the increase of the small fragments signal intensity. As it was the case for the M.A. and I.A. in the previous part, the presence of unsaturations limits the formation of the CH_3^+ fragments which suggest a lower degradation of the monomer. The $COOH^+$, signal associated with the function of interest, shows a similar trend which allows us to assume that the degradation of the acid function is limited in presence of the double bonds. This analysis also reveals the essential role of the distance between the C=C bond and the function of interest where the possible resonance between the double bond located in alpha of the acid group could be seen as a stabilizer of the function of interest limiting the fragmentation of the monomer. A relevant parameter to evaluate the stabilization within the acidic precursor is their pka value. In this study, the pka values of B.A., C.A. and Be.A. are respectively evaluated at 4.82, 4.17 and 4.34. This lowest pka value for C.A. indicates a stronger acidic character which is justified by the better stabilization of the conjugated base once deprotonated. On the contrary, the 4.82 pka value for B.A., without double bond, means a reduced acidic character and stabilization of the conjugated base. This strongly supports that the better preservation of the chemical structure with the position of the double bond is related to a resonance phenomenon and an intrinsic stabilization of the injected molecule.

3.2.2. Analysis of the plasma deposited coatings

The deposition rate and roughness of the deposited coatings is evaluated by stylus profilometry and reported in Fig. 14. The crotonic and 3-butenoic acid present higher deposition rates than the saturated butyric acid. Once again, the observed range of influence is very similar to fluorinated, acrylates and anhydrides monomers synthesized in a comparable DBD reactor. As reported earlier for anhydrides, this can be related to the different polymerization pathways between the unsaturated and saturated precursors. Also, the vapor pressure of each monomer, evaluated at 57, 25 and 60 Pa at 20 °C for B.A., C.A. and Be.A. respectively, is a good indication for either plasma polymerization in the gas phase or radical propagation at the surface. The recurrence of this phenomenon makes it a powerful tool for further investigations in fast synthesis of organic coatings since it does not seem to be dependent of the position of the double bond in the molecule but mostly associated to the presence of unsaturations. Roughness of the pd-coatings is compared for similar thicknesses. The critical difference between the saturated and unsaturated monomers is mainly related to the double polymerization pathway for crotonic and butanoic acid. Nevertheless, a slight difference is observed between these two molecules. This could be due to the filamentary character of the discharge which is more important in the case of the Be.A.. In fact, the electron density in the micro-discharges is known to be higher. This induces local and randomly dispersed privileged polymerization zones. The number of streamers being significantly higher with the injection of Be.A. rather than with C.A. could then be at the origin of this 10% roughness increase.

The essential role of the position of the double bond in the chemical preservation of the function of interest is evaluated by XPS and infrared spectroscopy. Since the three monomers only differ from each other by their amount of hydrogen, they present an identical C/O ratio (2.00). The elementary composition evaluated by XPS of the deposited coatings reveals a partial degradation of the initial structure of the precursor leading to an increase of the C/O ratio from 2.00 up to 5.23 ± 0.41, 4.5 ± 0.43 and 3.00 ± 0.38 for B.A., Be.A. and C.A. respectively. The strong amount of carbon in the butyric acid is not very surprising since its polymerization pathway is regulated by a fragmentation procedure. A clear correlation with the mass spectrometry measurements can be highlighted since the lightening of the plasma induced the most severe increase of the $COOH^+$ and CH_3^+ fragments. The trend in the general composition of the film is also observed in the XPS HR C1s spectra presented in the left part of the Fig. 15. The component associated with the acid function centered around 289.0 eV is clearly dependent on the presence of the unsaturation but also on the distance separating it from the unsaturation. The possible resonance of the C=C bond with the acid

function in the crotonic acid stabilizes the structure of the precursor and therefore favors the preservation of the initial structure of the precursor even in the highly energetic filamentary argon discharge. The chemical structure of the deposited films can easily be correlated to the MS measurements since the $COOH^+$ signal is more significantly increased with the Be.A. and the B.A. rather than C.A.. IRRAS measurements (right of the Fig. 15) confirm the preservation of the surface properties of the coatings in the bulk of the film. The 1.1 $COOH/CH_x$ ratio is indeed very low for the butyric acid because of the high fragmentation when compared to the initial 2.5 ratio of the monomer structure. A stronger preservation through the depth of the coating is observed with the presence of unsaturation, increasing the $COOH/CH_x$ ratio to 2.6 and 4.7 for Be.A. and C.A. respectively where their initial ratio is evaluated at 3.4 and 3.5. The protection of the function of interest is confirmed through an additional method and supports the resonance phenomenon between the sp^2 carbons of the C=C bond and the acid function.

4. Conclusion

In this paper, a method combining plasma phase analysis with the chemical properties of the deposited coatings is used for the fundamental understanding of the critical role of unsaturations in the plasma polymerization of organic coatings in atmospheric DBD systems. The effect of the presence of double bonds in the chemical structure of the injected precursor is highlighted through the use of methacrylate and isobutyric anhydride. Thanks to the identification of a "signature" fragment, a double polymerization pathway is proposed for the unsaturated monomer with a strong decrease of the filamentary character of the discharge. The combination of the plasma stabilization and the double polymerization pathway with the unsaturated monomer induced a dramatic increase of the deposition rate and a strong preservation of the function of interest because of the higher reactivity of the C=C bond. The influence of the distance between the double bond and the function of interest is discussed by the use of three monomers: butyric, crotonic and 3-butenoic acid. Similar trends as for the M.A. and I.A. were noted between the saturated and unsaturated precursors. On the other hand, no significant influence was noted on the deposition rate of the two unsaturated monomers. Anyhow, it suggests that the combination of a planar geometry and a resonance of the C=C bond located in alpha of the acid function could induce a strong preservation of the precursor structure through a severe limitation of its fragmentation.

Acknowledgements

The authors would like to thank the "Région Wallonne" for its financial support in the FLYCOAT project n°131847.

References

[1] R.D. Jerabek, J.R. Marchetti, Self-crosslinking cationic electrodepositable compositions, PPG Industries Inc., US Patent 3,922,253 (1974).
[2] P.J. Hazell, C. Stennett, G. Cooper, The shock and release behaviour of an aerospace-grade cured aromatic amine epoxy resin, Polym. Compos. 29 (2008) 1106–1110.
[3] L. Guadagno, M. Raimondo, V. Vittoria, L. Vertuccio, C. Naddeo, S. Russo, B. De Vivo, P. Lamberti, G. Spinelli, V. Tucci, Development of Epoxy Mixtures for Application in Aeronautics and Aerospace, Vol. 4 RSC Advances, 2014, pp. 15474–15488.
[4] C.P.R. Nair, Advances in addition-cure phenolic resin, Prog. Polym. Sc. 29 (2004) 401–498.
[5] N.N. Ghosh, B. Kiskan, Y. Yagci, Polybenzoxazines—New high performance thermosetting resins: synthesis and properties, Prog. Polym. Sc 32 (2007) 1344–1391.
[6] S.S. Pathak, A. Sharma, A.S. Khanna, Value addition to waterborne polyurethane resin by silicone modification for developing high performance coating on aluminum alloy, Prog. Org. Coat. 65 (2009) 206–216.
[7] Y. Wang, G. Xu, H. Yu, C. Hu, X. Yan, T. Guo, J. Li, Comparison of anti-corrosion properties of polyurethane based composite coatings with low infrared emissivity, App. Surf. Sc. 257 (2011) 4743–4748.
[8] J. Friedrich, Mechanisms of plasma polymerization-reviewed from a chemical point of view, Plasma Process. Polym. 8 (2011) 783–802.
[9] R.-S. Juang, C. Huang, H.-Y. Jheng, C. Li, L.-Y. Wu, Y.-J. Chang, Cyclonic plasma activation on microporous poly(vinyldiene fluoride) membranes for improving surface hydrophilicity, J, Taiwan Inst. Chem. Eng. 54 (2015) 76–82.
[10] N. De Geyter, R. Morent, C. Leys, L. Gengembre, E. Payen, Treatment of polymer films with a dielectric barrier discharge in air, helium and argon at medium pressure, Surf. Coatings Tech. 201 (2007) 7066–7075.
[11] A. Sarani, N. De Geyter, A. Nikiforov, R. Morent, C. Leys, J. Hubert, F. Reniers, Surface modification of PTFE using an atmsopheric pressure plasma jet in argon and argon + CO2, Surf. Coatings Technol. 206 (8–9) (2012) 2226–2232.
[12] V. Kumar, J. Pulpytel, G. Giudetti, H. Rauscher, F. Rossi, F. Arefi-Khonsari, Amphiphilic copolymer coatings via plasma polymerization process: Switching and anti-biofoulig characteristics, Plasma Process. Polym. 8 (2011) 373–385.
[13] M. Navarro-Rosales, C.A. Ávila-Orta, M.G. Neira-Velázquez, H. Ortega-Ortiz, E. Hernández-Hernández, S.G. Solís-Rosales, B.L. España-Sánchez, P. Gónzalez-Morones, R.M. Jímenez-Barrera, S. Sánchez-Valdes, P. Bartólo-Pérez, Effect of plasma modifications of copper nanoparticles on their antibacterial properties, Plasma Process. Polym. 11 (2014) 685–693.
[14] M. Drábik, O. Polonskyi, O. Kylián, J. Čechvala, A. Artemenko, I. Gordeev, A. Choukourov, D. Slavínská, I. Matolínová, H. Biederman, Super-hydrophobic coatings prepared by RF magnetron sputtering of PTFE, Plasma Process. Polym. 7 (2010) 544–551.
[15] Y.N. Kok, P.J. Kelly, Properties of pulsed magnetron sputtered TiO2 coatings grown under different megnetron configurations and power deliver moes, Plasma Process. Polym. 4 (2007) S299–S304.
[16] B. Nisol, G. Oldenhove, N. Preyat, D. Monteyne, M. Moser, D. Perez-Morga, F. Reniers, Atmospheric plasma synthesized PEG coatings: non-fouling biomaterials showing protein and cell repulsion, Surf. Coatings Technol. 252 (2014) 126–133.
[17] M. Aliofkhazraei, A.S. Rouhaghdam, E. Ghobadi, E. Mohsenian, Study of shape and distribution of TiO2 nanorods produced by atmospheric pressure plasma, Plasma Process. Polym. 6 (2009) 214–217.
[18] P. Heyse, R. Dams, S. Paulussen, K. Houthoofd, K. Janssen, P.A. Jacobs, B.F. Sels, Dielectric barrier discharge at atmospheric pressure as tool to deposite versatile organic coatings at moderate power input, Plasma Process. Polym. 4 (2007) 145–157.
[19] F. Hilt, D. Duday, N. Gherardi, G. Frache, J. Bardon, P. Choquet, Plasma deposition of an organophosphorus coating at atmospheric pressure, Plasma Process. Polym. 10 (2013) 556–563.
[20] C. De Vos, N. Vandencasteele, A. Kakaroglou, B. Nisol, I. De Graeve, G. Van Assche, B. Van Mele, H. Terryn, Plasma Polymerization of a saturated branched hydrocarbon. The case of heptamethylnonane, Plasma Process. Polym. 10 (2013) 51–59.
[21] X. Zhu, F. Arefi-Khonsari, C. Petit-Etienne, M. Tatoulian, Open air deposition of SiO2 films by an atmospheric pressure line-shaped plasma, Plasma Process. Polym. 2 (2005) 407–413.
[22] P.A. Premkumar, S.A. Starostin, H. de Vries, M. Creatore, P.M. Koenraad, W.A. MacDonald, M.C.M. van de Sanden, Surface dynamics of SiO2-like films on polymers grown by DBD assited CVD at atmospheric pressure, Plasma Process. Polym. 9 (2012) 1194–1207.
[23] J. Drews, H. Launay, C.M. Hansen, K. West, S. Hvilsted, P. Kingshott, K. Almdal, Hydrolysis and stability on thin pulsed plasma polymerised maleic anhydride coatings, Appl. Surf. Sci. 254 (2008) 4720–4725.
[24] J. Hu, C. Yin, H.-Q. Mao, K. Tamada, W. Knoll, Functionalization of poly(ethylene terephtalate) film by pulsed plasma deposition of maleic anhydride, Adv. Funct. Mater. 13 (2003) 692–697.
[25] G. Mishra, S.L. McArthur, Plasma polymerization of maleic anhydride: just what are the right deposition conditions, Langmuir 26 (2010) 9645–9658.
[26] M.E. Ryan, A.M. Hynes, J.P.S. Badyal, Pulsed plasma polymerization of maleic anhydride, Chem. Mater. 8 (1996) 37–42.
[27] A.N. Chifen, A.T.A. Jenkins, W. Knoll, R. Förch, Adhesion improvement of plasma-polymerized maleic anhydride films on gold using HMDSO/O-2 adhesion layers, Plasma Process. Polym. 4 (2007) 815–822.
[28] Y. Zhao, M.W. Urban, Spectroscopic studies of microave plasma reactions of maleic anhydride on poly(vynildiene fluoride) surfaces: crystalilinity and surface reactions, Langmuir 2 (1999) 3538–3544.
[29] H. Hody, P. Choquet, M. Moreno, J.-J. Pireaux, Optimization of an atmospheric pressure plasma copolymerization process with a view to nanopowder functionalization, Plasma Process. Polym. 6 (2009) S883–S887.
[30] A. Manakhov, M. Moreno-Couranjou, N.D. Boscher, V. Rogé, P. Choquet, J.-J. Pireaux, Atmospheric pressure pulsed plasma copolymerization of maleic anhydride and vinyltrimethoxysilane: influence of electrical parameters on chemistry, morphology and deposition rate of the coatings, Plasma Process. Polym. 9 (2012) 435–445.
[31] A. Manakhov, M. Michliecek, D. Necas, J. Polcak, E. Makhneva, M. Elias, L. Zajickova, Carboxyl-rich coatings deposited by atmospheric plasma co-polymerization of maleic anhydride and acetylene, Surf. Coat. Technol. 295 (2016) 37–45.
[32] C. Tarducci, W.C.E. Schofield, J.P.S. Badyal, S.A. Brewer, C. Willis, Synthesis of cross-linked ethylene glycol dimethacrylate and cyclic methacrylate anhydride polymer structures by pulsed plasma deposition, Macormol. 14 (2002) 8724–8727.
[33] G. Mertz, T. Fouquet, C. Becker, F. Ziarelli, D. Ruch, D. a methacrylate anhydride difunctional precursor to produce a hydrolysis-sensitive coating by aerosol-assisted atmospheric plasma process, Plasma Process. Polym. 11 (2014) 728–733.
[34] D. Hegemann, E. Körner, S. Guimond, Plasma polymerization of acrylic acid revisited, Plasma Process. Polym. 6 (2009) 246–254.
[35] B. Gupta, C. Plummer, I. Bisson, P. Frey, J. Hilborn, Plasma-induced graft

polymerization of acrylic acid onto poly(ethylene terephthalate) films: characterization and human smooth muscle cell growth on grafted films, Biomaterials 23 (2002) 863–871.
[36] A.P. Kettle, A.J. Beck, L. O'Toole, F.R. Jones, R.D. Short, Plasma polymerization for molecular engineering of carbon-fibre surfaces for optimized composites, Compo. Sc. Tech. 57 (1997) 1023–1032.
[37] L. Denis, D. Cossement, T. Godfroid, F. Renaux, C. Bittencourt, R. Snyders, M. Hecq, Synthesis of allylamine plasma polymer films: correlation between plasma diagnostic and film characteristics, Plasma Process. Polym. 6 (2009) 199–208.
[38] S. Ligot, M. Guillaume, P. Raynaud, D. Thiry, V. Lemaur, T. Silva, N. Britun, J. Cornil, P. Dubois, R. Snyders, Experimental and theoretical study of the plasma chemistry of ethyl lactate plasma polymerization discharges, Plasma Process. Polym. 12 (2015) 405–415.
[39] L. Denis, P. Marsal, Y. Olivier, T. Godfroid, R. Lazzaroni, M. Hecq, J. Cornil, R. Snyders, Deposition of functional organic thin films by pulsed plasma polymerization: a joint theoretical and experimental study, Plasma Process. Polym. 7 (2010) 172–181.
[40] B. Nisol, G. Arnoult, T. Bieber, A. Kakaroglou, I. De Graeve, G. Van Assche, H. Terryn, F. Reniers, About the influence of double bonds in the APPECVD of acrylate-like precursors: a mass spectrometry study of the plasma phase, Plasma Process. Polym. 11 (2014) 335–344.
[41] A. Kakaroglou, G. Scheltjens, B. Nisol, I. De Graeve, G. Van Assche, B. Van Mele, R. Willem, M. Biesemans, F. Reniers, H. Terryn, H. Deposition, Characterization of plasma polymerized allyl methacrylate based coatings, Plasma Process. Polym. 9 (2012) 799–807.
[42] A. Batan, B. Nisol, A.A. Kakaroglou, I. De Graeve, G. Van Assche, B. Van Mele, G.H. Terryn, F. Reniers, The impact of double bonds in the APPECVD of acrylate-like precursors, Plasma Process. Polym. 10 (2013) 857–863.
[43] J. Hubert, J. Mertens, T. Dufour, N. Vandencasteele, F. Reniers, P. Viville, R. Lazzaroni, M. Raes, H. Terryn, Synthesis and texturization processes of (super)-hydrophobic fluorinated surfaces by atmsopheric plasma, J. Mater. Res. 30 (2015) 3177–3191.
[44] K. Yamada, H. Yamane, K. Kumada, S. Tanabe, T. Kajiyama, Plasma-graft polymerization of a monomer with double bonds onto the surface of carbon fiber and its adhesion to a vinyl ester resin, J. Appl. Polym. Phys. 90 (2003) 2415–2419.
[45] J. Hubert, N. Vandencasteele, J. Mertens, P. Viville, T. Dufour, C. Barroo, T. Visart de Bocarmé, R. Lazzaroni, F. Reniers, Chemical and physical effects of the carrier gas on the atmospheric pressure PECVD of fluorinated coatings, Plasma Process. Polym. 12 (2015) 1174–1185.
[46] A. Ozkan, T. Dufour, T. Silva, N. Britun, R. Snyders, A. Bogaerts, F. Reniers, The influence of power and frequency on the filamentary behavior of a flowing DBD-application to the splitting of CO2, Plasma Sources Sc. Tech. 25 (2016) (025013).
[47] T. Manley, The electric characteristics of the ozonator discharge, J. Electrochem. Soc. 84 (1943) 83–96.
[48] J. Hubert, C. Poleunis, A. Delcorte, P. Laha, J. Bossert, S. Lamberts, A. Ozkan, P. Bertrand, H. Terryn, F. Reniers, Plasma polymerization of C_4Cl_6 and $C_2H_2Cl_4$ at atmospheric pressure, Polym. 54 (2013) 4085–4092.
[49] B. Qi, J. Huang, L. Gao, Y. Qiu, Electron density measurements in an atmospheric pressure argon discharge by means of plasma radiation, Phys. Plasmas 16 (2009) 083301.
[50] U. Kogelschatz, Dielectric-barrier discharges: their history, discharge physics, and industrial applications, Plasma Chem. Plasma Process. 23 (2003) 1–46.
[51] B. Nisol, H. Gagnon, S. Lerouge, M.R. Wertheimer, Energetics of reactions in atmospheric-pressure plasma polymerization with inert carrier gas, Plasma Process. Polym. 13 (2016) 366–374.
[52] B. Nisol, S. Watson, S. Lerouge, M.R. Wertheimer, Energetics of reactions in a dielectric barrier discharge with argon carrier gas: V Hydrocarbons, Plasma Process. Polym. 14 (2017) 1600191 (9p).
[53] B. Nisol, S. Watson, S. Lerouge, M.R. Wertheimer, Energetics of reactions in a dielectric barrier discharge with argon carrier gas: III esters, Plasma Process. Polym. 13 (2016) 900–907.
[54] L.G. Piper, W.C. Richardson, G.W. Taylor, D.W. Setser, Faraday Diss, Chem. Soc. 53 (1972) 100–110.
[55] L.G. Piper, J.E. Velazco, D.W. Setser, J. Chem. Phys. 59 (1973) 3323–3340.
[56] F. Loyer, G. Farche, P. Choquet, N.D. Boscher, Atmospheric pressure Plasma-Initiated Chemical Vapour Deposition (AP-iCVD) of Poly(alkylacrylates): an Experimental Study, Macromolecules 50 (2017) 4351–4362.
[57] F. Loyer, F. Bengasi, G. Farche, P. Choquet, N.D. Boscher, Insights in the initiation and termination of poly(alkyl acrylates) synthesized by atmospheric pressure plasma-initiated chemical vapor deposition (AP-iCVD), Plasma Process. Polym. 15 (2018) 1800027 (10p).
[58] F. Loyer, S. Bulou, P. Choquet, N.D. Boscher, Pulsed plasma initiated chemical vapor desposition (PiCVD) of polymer layers – a kinetic model for the description of gas phase to surface interactions in pulse plasma discharges, Plasma Process. Polym. (2018), https://doi.org/10.1002/ppap.201800121 Current inclusion in an issue.
[59] S.J. Blanksby, G.B. Ellison, Bond dissociaton energies of organic molecules, Acc. Chem. Res. 36 (2003) 255–263.
[60] V. Hrachovà, A. Kaoka, Study of the admixture influence on the oxygen spectra properties, Vacuum 48 (1997) 689–692.
[61] S.-Z. Li, W.-T. Huang, J. Zhang, D. Wang, The effect of gas flow on argon plasma discharge generated with a single-electrode configuration at atmospheric pressure, Appl. Phys. Lett. 94 (2009) 111501.
[62] Q. Xiong, A.Y. Nikiforov, L. Li, P. Vanraes, R. Snyders, X.P. Lu, C. Leys, Absolute OH density determination by laser induced fluorescence spectroscopy in an atmospheric pressure RF plasma jet, Eur. Phys. J. D 66 (2012) 281.